function in the SNpc can lead to novel PD treatments. There are four types of glial cells in the SNpc: astrocytes, microglia, oligodendrocytes, and NG2 glia. The NG2 glia are glial cells specifically expressing NG2 chondroitin sulphate proteoglycan, and are, at least in part, precursor cells for oligodendrocytes. NG2 glia are sometimes also called NG2 cells, synantocytes, and polydendrocytes (Butt et al. 2005; Staugaitis and Trapp 2009; Trotter et al. 2010).

In response to neuronal injuries, astrocytes become activated, increase their expression of glial fibrillary acidic protein (GFAP), and migrate to the sites of injury. At this point, they are called reactive astrocytes, and form astroglial scars in and around the injury sites. In PD, the accumulation of reactive astrocytes in the SNpc is well documented (McGeer and McGeer 2008; Asanuma et al. 2010; Choudhury et al. 2011). Although the actions of reactive astrocytes on neuronal survival have not yet been fully elucidated, it is believed that they possess neuroprotective attributes, which have mainly been observed in *in vitro* experiments (Tanaka et al. 1999; Miyazaki et al. 2011). The neuroprotective actions of astrocytes have been attributed to their antioxidant defense mechanisms, and their ability to secrete a variety of neuroprotective factors, such as glial cell-line-derived neurotrophic factor (GDNF) (Schaar et al. 1993) and brain-derived neurotrophic factor (BDNF) (Dreyfus et al. 1999). Because of the presumed neuroprotective role of astrocytes, agents targeting these cells have been proposed to suppress DArgic neurodegeneration (Asanuma et al. 2010; Choudhury et al. 2011).

Microglia play pivotal roles in immune reactions in the brain. Microglial cells are mesodermal in origin with macrophage-like properties (Kreutzberg 1996). PD has some features in common with neuroinflammatory diseases, because it is characterized by the presence of activated microglia in the SNpc (Mosley et al. 2006; McGeer and McGeer 2008; Long–Smith et al. 2009; Tansey and Goldberg 2010). Similar neuroinflammatory reactions may be critical in another major neurodegenerative disorder Alzheimer's disease (Lue et al. 2010) and therefore microglia should be the therapeutic targets to suppress neurodegeneration (Yacoubian and Standaert 2009). However, in contrast to astrocytes, the majority appears to support the notion that microglia are detrimental to the disease (Liberatore et al. 1999; Block et al. 2007; Henry et al. 2009; Marinova–Mutafchieva et al. 2009), as they are known to produce proinflammatory cytokines, such as interleukin-1β (IL-1β) and tumor necrosis factors α (TNFα) (Long–Smith et al. 2009; De Lella Ezcurra et al. 2010), and increase oxidative stress (Liberatore et al. 1999; Levesque et al. 2010). Thus, astrocytes and microglia have often been implicated in the pathogenesis of PD. On the other hand, NG2 glia and oligodendrocytes have also been shown to abundantly exist in the SNpc, whereas very little is known about their roles in PD (McGeer and McGeer 2008).

A cytokine mixture of granulocyte macrophage colony-stimulating factor (GM-CSF) and IL-3 has been found of its much stronger ameliorative effect on the stab-wounded rat brains than the solely used GM-CSF or IL-3 (Nishihara et al. 2011). In the present study, the cytokine mixture effectively prevented 6-hydroxydopmaine (6-OHDA)-induced neurodegeneration in the SNpc, which is an animal model of Parkinsonism. The findings suggest that the effects are mediated by increased expression of prosurvival proteins, and the differential activities of neuroinflammatory cells, including NG2 glia, whose role may be implicated in neuronal survival.

Materials and Methods

Animals

Adult male Wistar rats, weighing 220–250 g, were housed under standard laboratory conditions. The animals were allowed free access to food and water throughout the experiments. The rats were kept in a 12/12 h dark/light cycle. All animal experiments were carried out in accordance with the Guidelines for Animal Experimentation of Ehime University Graduate School of Medicine.

6-OHDA treatment and cytokine injection

Animals were kept under pentobarbital sodium anesthesia (50 mg/kg) and placed in a stereotactic instrument (Narishige, Tokyo, Japan). 6-OHDA (Sigma, St. Louis, MO) was dissolved in saline containing ascorbic acid (Wako, Osaka, Japan) (10 μg/μL dissolved in 1% ascorbate-saline), kept on ice (4°C) and protected from light to minimize oxidation, until use. The rats were then given uni- or bilateral injections of 6-OHDA. Unilateral injection was employed for immunohistochemical analyses, and bilateral injection was used for all other studies. For unilateral injection, 5 μL of 6-OHDA was drawn into a Hamilton syringe and then injected into the right side of the striatum, through a hole made on the skull at 1 mm anterior to bregma and 3 mm lateral from the midline. The depth of the needle tip was 5 mm from the skull surface. The same amount of 6-OHDA was injected into the left side of the striatum for bilateral injection. The rate of fluid injection was 1 μL /min. The needle was left at the point of injection for an additional 10 min after the injection and then slowly withdrawn. Because the bilaterally injected rats could not move well to drink or to eat, they were intraperitoneally injected with electrolyte solution (Solita-T3, Ajinomoto, Tokyo, Japan) twice per day for 1 week. A cytokine mixture containing 0.2 mg/mL rat recombinant GM-CSF (PeproTech, London, UK) and 0.2 mg/mL rat recombinant IL-3 (PeproTech) was subcutaneously injected from the next day of the 6-OHDA-treatment at a dose of 10 μg/kg body weight (Nishihara et al. 2011). For the control, the same amount of saline was subcutaneously injected.

© 2011 The Authors. Published by Wiley Periodicals, Inc.

Determination of DA content in the striatum

The DA content in the striatum was measured by high-performance liquid chromatography (HPLC) (Yabe et al. 2009). Both sides of the striatum were dissected out and quickly put on an ice-cold glass plate and stored at −80°C until assayed. The striatum samples from both sides were independently homogenized with an ultrasonic cell disruptor (Tomy Seiko, Tokyo, Japan) in 0.1 M perchloric acid containing 5 mM EDTA (Wako) and 3,4-dihydroxybenzamine (Wako), and were centrifuged. A 10-μL aliquot of the filtered supernatant was injected into a HPLC apparatus with a reversed-phase column. The mobile phase consisted of 15% (v/v) methanol containing 0.1 M sodium acetate (Wako) and 0.1 M citric acid (Wako), adjusted to pH 3.5, with 180 mg/L sodium octydyl sulphate (Wako), and 10 mM EDTA, pumped through the column at a rate of 0.25 mL/min. The data from the right and left striatum were averaged and processed for statistical analysis.

Rota-rod test

Motor coordination and balance were tested using a rota-rod (Ugo Basile, Rota-rod 7750, Italy) before administration of drugs, and 7, 14, 21, 28, and 56 days after administration of the drugs. The rota-rod test was performed by placing the rat on a rotating drum and measuring the time each animal was able to maintain its balance while attempting to walk on top of the rod (Dekundy et al. 2007). The test was done between 1400 h and 1500 h. Animals were pretrained twice a day, 3 days before the test. The speed of the rota-rod was maintained fixed at 40 rpm over a 300-s period. The animals were touched on their tails several times in each session to maintain a high degree of alertness in the test. The rota-rod performance was expressed in seconds; namely the amount of time the animals remained on the rotating rod.

Quantitative real-time reverse transcriptase-polymerase chain reaction (qRT-PCR)

The right side ventral midbrain containing the substantia nigra (midbrain delineated longitudinally 4.5 to 6.6 mm from bregma, perpendicularly under 7 mm from the skull) was dissected out at 7 days after 6-OHDA-treatment and stored at −80°C until assayed. Tissue samples were homogenized in ISOGEN (Nippon gene, Tokyo, Japan) using an ultrasonic cell disruptor. Then, their total RNA was collected. cDNA was obtained from DNase-I-treated RNA by reverse transcription using an oligo-(dT) 15 primer, as previously described (Takahashi et al. 2008). cDNA samples were prepared from seven separate samples of brain tissue astrocytes and microglia. Quantitative real-time reverse transcriptase PCR (qRT-PCR) analysis was performed in triplicate using a MJ mini instrument (BioRad, Hercules, CA) using Fast Start Universal SYBR Green (Roche Diagnostic Japan, Tokyo, Japan). PCR conditions were as follows: 50°C for 2 min, 95°C for 10 min, followed by 40 cycles of 95°C for 15 s and 60°C for 1 min. All gene-specific mRNA expression values were normalized against β-actin mRNA. The primer sequences for each gene, as well as the sizes of their products, are listed in Table 1.

Table 1. **Oligonucleotide primers for real-time RT-PCR**

Gene	Sense/anti-sense
β-Actin	5′-AGA AGA GCT ATG AGC TGC CTG ACG-3′
	5′-TAC TTG CGC TCA GGA GGA GCA ATG-3′
TH	5′-TGT GTC CGA GAG CTT CAA TG-3′
	5′-GGG CTG TCC AGT ACG TCA AT-3′
Iba1	5′-GTC CTT GAA GCG AAT GCT GG-3′
	5′-CAT TCT CAA GAT GGC AGA TC-3′
NG2	5′-TTA CCT TGG CCT TGT TGG TC-3′
	5′-GAT GAT CTG TTT GGC CTG CT-3′
PCNA	5′-TAA GTT GTC CCA GAC AAG CA-3′
	5′-GCG ATC GTC AAA GGT TTA GT-3′
GFAP	5′-CAG AAG CTC CAA GAT GAA ACC AA-3′
	5′-TCT CCT CCT CCA GCG ACT CAA C-3′
IGF-1	5′-TTG CGG GGC TGA GCT GGT GGA C-3′
	5′-GCG GTG ACG TGC CAT TTT CTG TTC-3′
HGF	5′- TCT TGG TGT CAT TGT TCC TG -3′
	5′-CCA TGG ATG CTT CAA ATA CA -3′
BDNF	5′-CGT GAT CGA GGA GCT GTT GG-3′
	5′-CTG CTT CAG TTG GCC TTT CG-3′
GM-CSFRα	5′-ACT AGT ATG TGG CTG CAG AAT TTA CTT TTC-3′
	5′-GGT ACC TCA TTT CTG GAC CGG CTT CC-3′
IL-3Rα	5′-ACT AGT ATG GTT CTT GCC AGC TCT AC-3′
	5′-GGT ACC TTA ACA TTC CAC GGT CAT AGG G-3′
Metallothionein 2	5′-CAC AGA TGG ATC CTG CTC CT-3′
	5′-GAG AAC CGG TCA GGG TTG TA-3′
Cu/Zn SOD	5′-TTC GAG CAG AAG GCA AGC GG-3′
	5′-ATC CCA ATC ACA CCA CAA GC-3′
Bcl-xL	5′-CCT ATC TTG GCT TTG GAT CC-3′
	5′-TTT CTT CTG GGG CTT CAG TC-3′
Bax	5′-TGC AGA GGA TGA TTG CTG AC-3′
	5′-GAT CAG CTC GGG CAC TTT AG-3′
TNFα	5′-CCC AGA CCC TCA CAC TCA GAT-3′
	5′-TTG TCC CTT GAA GAG AAC CTG-3′
IL-1β	5′-CAC CTT CTT TTC CTT CAT CTG T-3′
	5′-GTC GTT GCT TGT CTC TCC TTG TA-3′

TH = tyrosine hydroxylase; PCNA = proliferating cell nuclear antigen; GFAP = glial fibrillary acidic protein; IGF-1 = insulin-like growth factor-1; HGF = hepatocyte growth factor; BDNF = brain-derived neurotrophic factor; Cu/Zn SOD = copper and zinc superoxide dismutases; TNFα = tumor necrosis factor α; GM-CSFRα = granulocyte macrophage colony-stimulating factor receptor α; IL = interleukin.

Immunoblotting

The ventral midbrain from the opposite side of the tissue used for qRT-PCR (n = 7) was immediately homogenized with SDS solution in 10 volumes of Laemmli's

© 2011 The Authors. Published by Wiley Periodicals, Inc.

Table 2. **Primary antibodies used in this study**

Antigen	*Antibody*	*Dilution*	*Source*
β-actin	Mouse monoclonal	1:1000	Sigma
TH	Sheep polyclonal	1:500	Gene tex
TH	Rabbit polyclonal	1:500	abcam
Iba1	Rabbit polyclonal	1:500	Wako
NG2	Mouse monoclonal (132.39)	1:500	Chemicon
GFAP	Rabbit polyclonal	1:500	SHIMA Laboratories
CD11b	Mouse monoclonal (MRC OX42)	1:250	Serotec
Bcl-xL	Mouse monoclonal	1:100	Transduction Laboratories
TNF-α	Rabbit polyclonal	1:500	Santa Cruz
GM-CSFRα	Rabbit polyclonal	1:500	Santa Cruz
IL-3Rα	Rabbit polyclonal	1:500	Santa Cruz
TNF-α	Rabbit polyclonal	1:100	Bioworld Technology, Inc.
IL-1β	Rabbit polyclonal	1:100	Bioworld Technology, Inc.

TH = tyrosine hydroxylase; GFAP = glial fibrillary acidic protein; TNFα = tumor necrosis factor α; GM-CSFRα = granulocyte macrophage colony-stimulating factor receptor α; IL = interleukin.

sample solution containing 3% sodium dodecyl sulfate (SDS). The lysates were electrophoresed, transferred to nitrocellulose membranes, and immunoblotted with antibodies to β-actin, tyrosine hydroxylase (TH), Iba1, NG2, and Bcl-xL (Table 2). The immunoreaction was visualized using nitro blue tetrazolium and 5-bromo-4-chloro-3-indolyl phosphate, as described previously (Tanaka et al. 1998). Immunoreactive bands were analyzed by densitometry using ImageJ 1.43u (Wayne Rasband, National Institute of Health, Bethesda, ML). The densitometry data were standardized with the internal standard β-actin.

Immunohistochemical staining

The primary antibodies listed in Table 2 were used for indirect immunofluorescence staining (Yokoyama et al. 2006). Briefly, anesthetized rats were fixed by transcardially perfusing 4% paraformaldehyde containing 2 mM $MgCl_2$ for 10 min, at a flow rate of 80 mL/min. The dissected brains were immersed in 15% sucrose in PBS at 4°C overnight, rapidly frozen in dry ice powder, and sliced into 10-μm thick coronal sections at the substantia nigra level (from bregma 4.80 mm to 5.40 mm). The brain sections were incubated with the primary antibodies followed by incubation with DyLight 488, DyLight 549, and/or DyLight 649-labeled secondary antibodies (Jackson ImmunoResearch Laboratories, West Grove, PA). Hoechst 33258 (Sigma) was used for nuclear staining. The immunostained specimens were observed with a Nikon A1 confocal laser scan microscope (CLSM; Tokyo, Japan) using 20× or 60× objective lenses. The area observed was 2.0–2.3 mm lateral from the midline.

Morphometric analysis

Brain sections processed as described above were triple-immunostained with antibodies to Iba1, TH, and NG2. To determine the area occupied by DArgic neurons, microglia, and NG2 glia, and also their overlapping area in the SNpc of the sections, micrographs were taken with the CLSM using a 20× lens. The images were processed using Adobe Photoshop CS5 Extended (Adobe Systems, San Jose, CA) and ImageJ 1.43u. First, the area where the DArgic neurons in the SNpc were distributed was demarcated as the SNpc. Then, the SNpc was further subdivided based on immunostaining for TH, Iba1, and NG2. Overlapping staining for TH and Iba1, TH and NG2, Iba1 and NG2, and Iba1-positive, but NG2-negative, were serially determined (see Fig. 6). Data from five sham or six 6-OHDA-treated rats were statistically analyzed.

Primary cultures

Rat primary microglial cultures were prepared (Tanaka et al. 1998). Briefly, whole forebrains from neonatal rats were dissected out and dissociated into individual cells with a nylon bag with 160 μm pores. The dissociated cells were cultured as a mixed glial cell culture in 75 cm^2 flasks with 10% foetal calf serum-supplemented Dulbecco's modified Eagle's medium. Eleven or 14 days later, microglial cells were obtained from the mixed glial culture. The purity of the microglial culture was >99%, as determined by immunocytochemical staining using antibodies to GFAP and Iba1. For immunocytochemical detection of cytokine receptors, the cells were seeded onto poly-L-lysine-coated glass coverslips placed in four-well culture plates, and then immunostained for GM-CSF and IL-3 receptors, as described above. Micrographs were taken with conventional optics using an Olympus BX-52 (Olympus, Tokyo, Japan). qRT-PCR to detect microglial mRNAs was performed in the same way as described above.

Statistical analysis

Numerical data expressed as means ± SEM were statistically analyzed using InStat3 software (GraphPad Software, La Jolla, CA). Statistical significance was assessed with one-way analysis of variance (ANOVA) and Tukey's *post hoc* test.

Results

Ameliorative effects of the cytokine mixture on motor function in 6-OHDA-induced Parkinsonian rats

The rats that received bilateral administration of 6-OHDA into the striatum did not move smoothly, and had difficulty in eating and drinking. Such motor dysfunction was apparent 6 h after 6-OHDA administration. As a result, rat body weights only minimally increased 7 days after 6-OHDA administration (Fig. 1A). After this time point, however, the

© 2011 The Authors. Published by Wiley Periodicals, Inc.

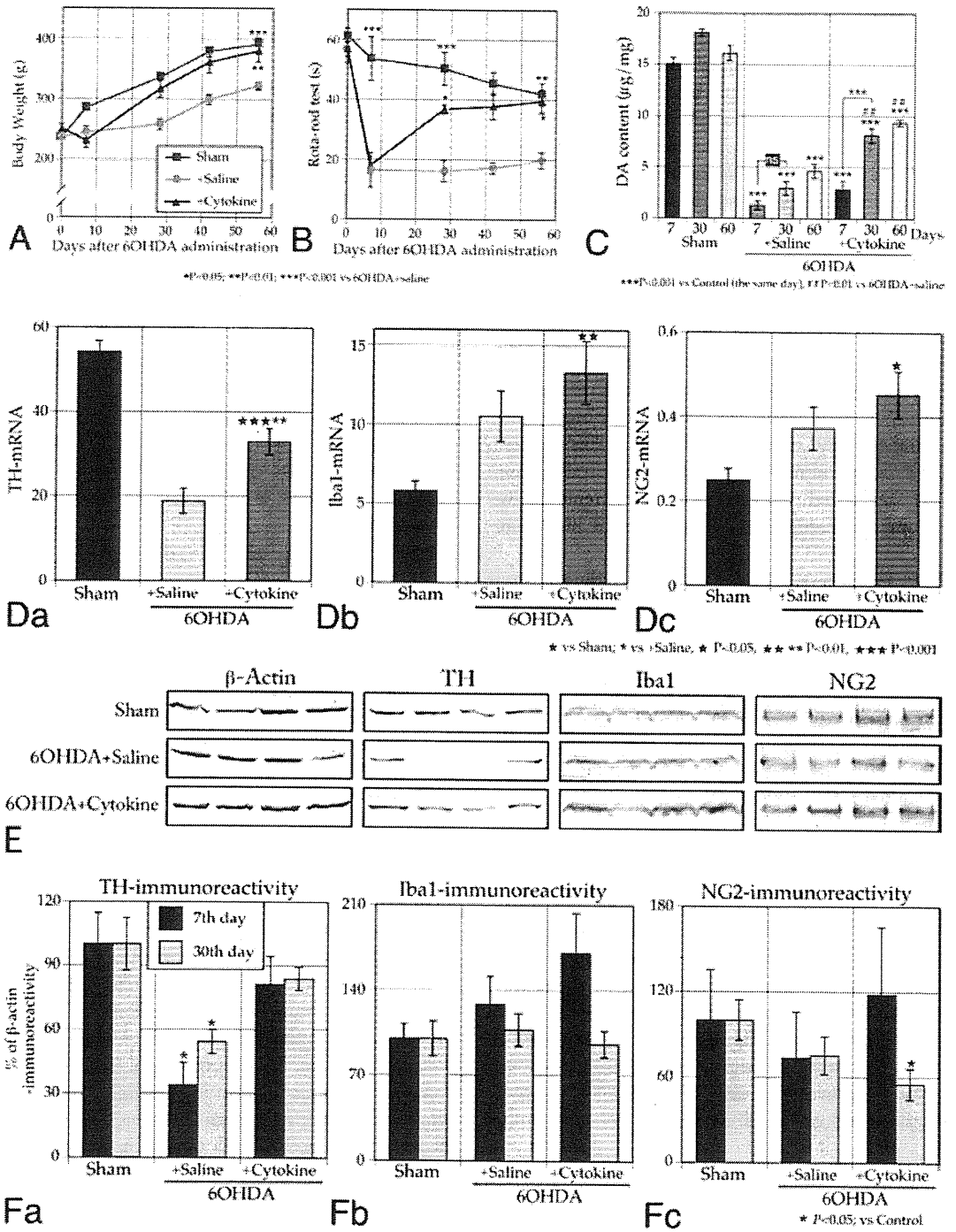

Figure 1. Effects of subcutaneous injection of the cytokine mixture on 6-OHDA-induced Parkinsonian rats. 6-OHDA was bilaterally administered into the striatum. +Saline or +Cytokine indicate 6-OHDA-administred rats with subcutaneous injection of saline or cytokine, respectively. Subcutaneous injection of the cytokine mixture was started 1 day after 6-OHDA administration, and repeated seven times (once per day). (**A**) Body weight change during the course of 2 months after 6-OHDA administration; n = 21, 21, 14, 7, and 7, at 0, 1, 4, 6, and 8 weeks, respectively, after 6-OHDA administration. (**B**) Motor function was evaluated by rota-rod test. (**C**) DA content in the striatum was determined by HPLC. The bilateral data were averaged and expressed as means ± SEM. (**D**) Levels of mRNAs encoding TH, Iba1, and NG2 in the SNpc at 1 week from seven rats, as determined by qRT-PCR. (**E**) Representative immunoblot data (n = 4) showing TH, Iba1, NG2, and β-actin protein level at 1 week. (**F**) Densitometric analyses of the immunoblot data expressed as means ± SEM.

© 2011 The Authors. Published by Wiley Periodicals, Inc.

6-OHDA-lesioned rats that received the cytokine mixture injection (cytokine group) had increased body weight, nearly equivalent to the control animals' (sham group) body weights, and the body weights of the cytokine group rats were significantly greater than the lesioned rats that received saline injection (saline group). The rota-rod test revealed marked motor dysfunction of the 6-OHDA-treated groups at 1 week (Fig. 1B). However, the cytokine group recovered motor function at 4 weeks and later. The sham group had gradually declining motor function, probably due to their increasing bodyweights. Consequently, there were no differences in motor function between the sham and cytokine groups at 8 weeks.

DA levels were measured by HPLC in the striatum. Approximately 15 μg/mg tissue weight of DA was detected in the striatum of the sham group, but less than 3 μg/mg DA was present in the 6-OHDA-treated rats (Fig. 1C). This marked decrease in DA content may underlie the motor dysfunction of the 6-OHDA-treated rats. However, DA contents of the cytokine group increased to 8 μg/mg or more, at 30 days or later.

Total RNA was prepared from the ventral midbrain containing the SNpc and then reverse transcribed into cDNA for qRT-PCR (Fig. 1D). Although 6-OHDA administration decreased the amount of mRNA encoding the rate-limiting enzyme for DA synthesis TH, the mRNA level was higher in the cytokine group than in the saline-treated group (Fig. 1Da). mRNAs for the microglia marker Iba1 and the oligodendrocyte progenitor cell marker NG2 chondroitin sulphate proteoglycan (NG2) increased in the cytokine group.

Protein samples were prepared at 7 and 30 days after 6-OHDA treatment and used for immunoblotting to estimate the amount of TH, Iba1, and NG2 at the protein level in the SNpc. Representative results from four separate samples are shown in Fig. 1E. β-actin was used as an internal standard. The protein bands from seven separate samples were analyzed by scanning densitometry. Fig. 1F shows that the TH protein decreased in the saline-treated group compared with the sham group (Fig. 1Fa). Iba1 protein tended to increase in the cytokine group at 7 days, but the level returned to the sham level at 30 days (Fig. 1Fb). NG2 protein was significantly reduced at 30 days in the cytokine group (Fig. 1Fc).

Expression of GM-CSF and IL-3 receptors in neurons and microglia

Antibodies to GM-CSF receptor α (GM-CSFRα) and IL-3 receptor α (IL-3Rα) were used in combination with antibodies for TH, and a marker for microglia, CD11b, to investigate localization of these receptors in the SNpc (Fig. 2). GM-CSFRα-immunoreactivity was localized both in CD11b$^+$ microglia and the TH$^+$ DArgic neurons (Fig. 2A). However, some microglia appeared to express the receptor more strongly than neurons. IL-3Rα immunoreactivity was also localized in both microglia and DArgic neurons (Fig. 2B), but this immunoreactivity was stronger in the neurons than in microglia. Primary cultured microglial cells expressed both receptors (Fig. 2C, D). mRNAs encoding these receptors were evaluated by qRT-PCR. Both mRNAs were detected in the ventral midbrain (Fig. 2E). Only GM-CSFRα-mRNA significantly increased in response to cytokine injection in the 6-OHDA-treated rats. This increase may imply that GM-CSFR expression is regulated in a positive-feedback manner, while IL-3R expression may likely be in a negative-feedback manner. Therefore, when simultaneously injected, GM-CSF might more effectively work than IL-3. Cultured microglial cells also expressed both mRNAs (Fig. 2F). Given the high level of expression of GM-CSFRα-mRNA in the cultured microglia, it is likely that the main source of GM-CSFRα-mRNA in the ventral midbrain is microglia. On the other hand, DArgic neurons may be the main source of IL-3Rα-mRNA.

Increased expression of Bcl-xL in DArgic neurons in the SNpc of the cytokine-injected rats

Both GM-CSF and IL-3 have been reported to increase the expression of antiapoptotic factors belonging to the Bcl-2 family in isolated neurons (Wen et al. 1998; Huang et al. 2007; Schabitz et al. 2008). Immunohistochemical staining with antibodies to Iba1, TH, and Bcl-xL revealed that Bcl-xL immunoreactivity was localized to capillary-like structures (yellow arrowheads) in and around the SNpc in a sham rat (Fig. 3A). Bcl-xL-immunoreactivity was similarly localized in a saline-injected Parkinsonian rat, although the immunoreactivity was markedly suppressed (Fig. 3B). By contrast, strong Bcl-xL-immunoreactivity was localized to DArgic neurons of a cytokine-injected rat (Fig. 3C, blue arrowheads). Note that the activated morphology of microglia was found in the SNpc, only in the ipsilateral side of the 6-OHDA-treated rats. Furthermore, immunoreactivity at a similar level was observed in DArgic neurons in the contralateral SNpc of the cytokine-injected rat, where microglia display resting ramified morphology (Fig. 3D). qRT-PCR showed a significant increase of Bcl-xL-mRNA in the cytokine group (Fig. 3E), and the proapoptotic factor Bax-mRNA did not significantly change among the three groups (Fig. 3F). In comparison with the mRNA data, Bcl-xL protein was not increased in the cytokine group compared with the sham group. However, the Bcl-xL protein was markedly decreased in the saline group (Fig. 3G). These data suggest that 6-OHDA administration accelerates degradation of Bcl-xL protein and that the cytokine injection increased the transcription of Bcl-xL mRNA in DArgic neurons.

© 2011 The Authors. Published by Wiley Periodicals, Inc.

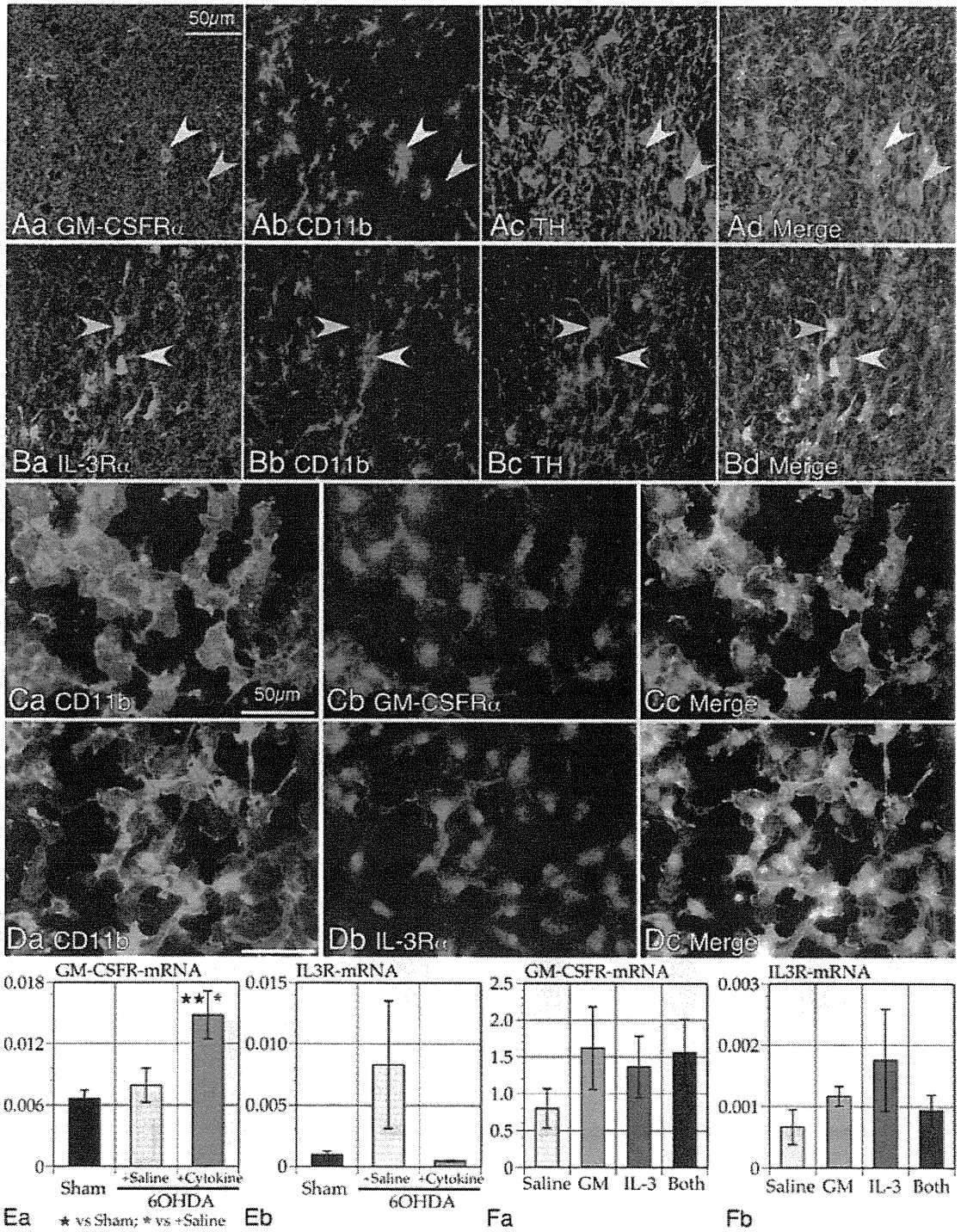

Figure 2. Expression of receptors for GM-CSF and IL-3 in the SNpc and primary cultured microglia. (**A**) Immunoreactivity of GM-CSFRα was localized to microglial cells (yellow arrowheads) and DArgic neurons (blue arrowheads). Microglial cells were identified with anti-CD11b antibody (OX42) and DArgic neurons with anti-TH-antibody. (**B**) Immunoreactivity of IL-3Rα was also localized to microglial cells (yellow arrowheads) and DA neurons (blue arrowheads). (**C** and **D**) Primary cultured microglial cells expressing GM-CSFRα (**C**) and IL-3Rα (**D**). (**E**) qRT-PCR revealed the presence of mRNAs encoding the receptors. The data from seven rats are expressed as means ± SEM. (**F**) The receptor mRNAs were expressed in the primary microglia culture. The data from 4 separate cultures are expressed as means ± SEM.

© 2011 The Authors. Published by Wiley Periodicals, Inc.

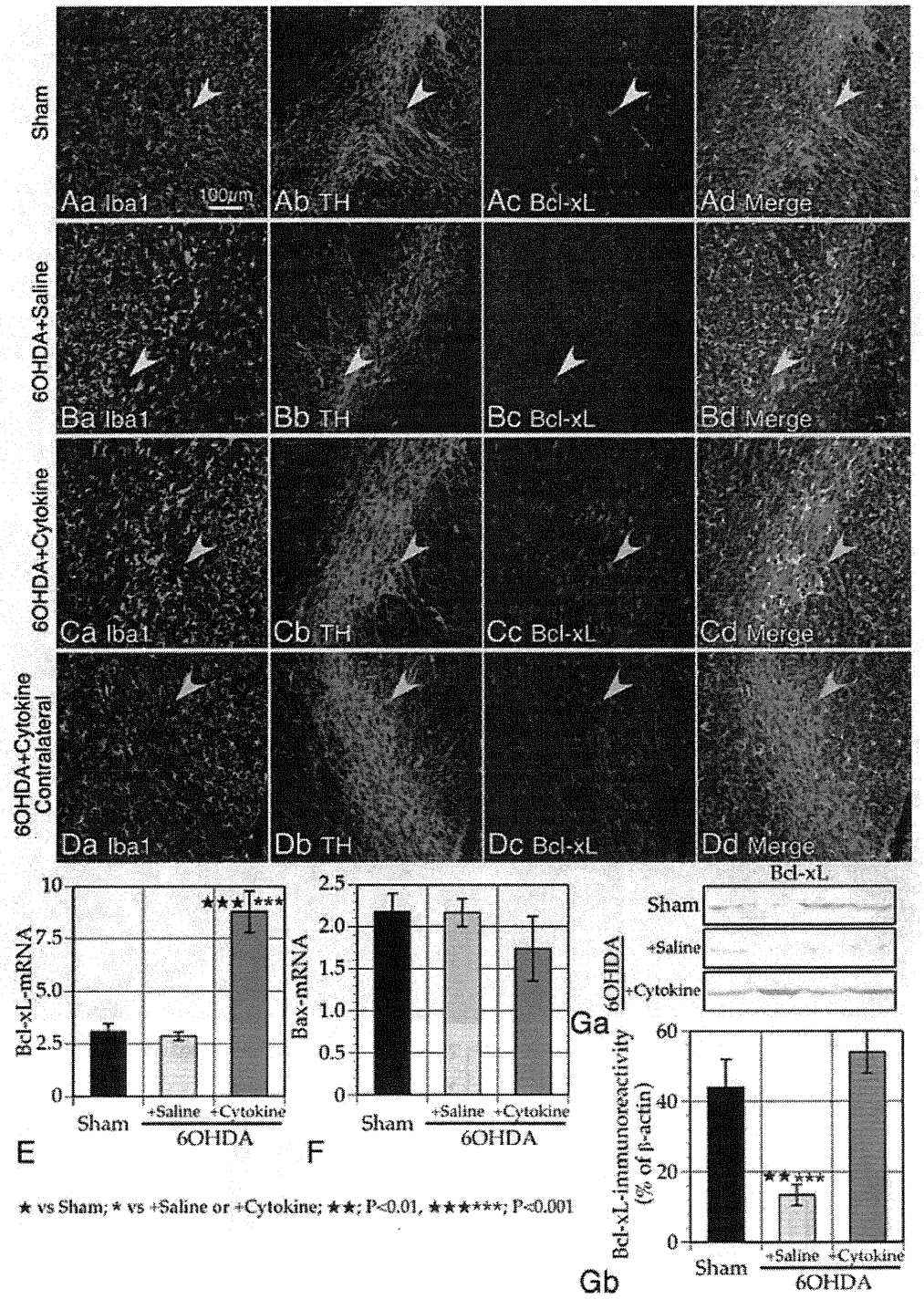

Figure 3. Antiapoptotic factor Bcl-xL expression in the SNpc. (**A–D**) Representative immunohistochemical data showing expression of Bcl-xL protein in the SNpc of sham, saline, and cytokine group at 1 week after 6-OHDA administrations. Localization of Bcl-xL immunoreactivity was only found in the cytokine-injected rat SNpc. The upregulated Bcl-xL expression was also found in the contralateral SNpc, where microglia display the resting phenotype. (**E**) Bcl-xL mRNA level was elevated in the cytokine group at 1 week, as revealed by qRT-PCR ($n = 7$). (**F**) Bax-mRNA did not show marked differences among the three groups. (**Ga**) Bcl-xL protein was strongly detected in the cytokine group by immunoblotting, while its expression was suppressed in the saline group. Representative data from four rats of each group are shown. (**Gb**) Densitometric analysis showed a significant drop in Bcl-xL protein expression in the saline group. Data from seven rats of each group are expressed as means ± SEM.

© 2011 The Authors. Published by Wiley Periodicals, Inc.

Phenotypic changes of microglia in response to the cytokines

It has been shown previously that primary cultured rat microglial cells change their morphology in response to GM-CSF and IL-3 (Fujita et al. 1996). To determine whether primary microglial cells change their functional phenotypes in response to the cytokines, total RNA was prepared from microglial cells cultured in the presence or absence of the cytokines, and mRNA levels encoding insulin-like growth factor-1 (IGF-1), hepatocyte growth factor (HGF), IL-1β, and TNFα were determined (Fig. 4A). Both IGF-1 and HGF ameliorate 6-OHDA-induced Parkinsonism (Clarkson et al. 2001; Koike et al. 2006; Ebert et al. 2008). mRNAs encoding the neuroprotective factors IGF-1 and HGF increased, and mRNAs for the detrimental proinflammatory cytokines decreased in the presence of the both cytokines. Thus, this result indicates that GM-CSF and IL-3 strengthened the neuroprotective nature of cultured microglia. Similar results were obtained in *in vivo* experiments (Fig. 4B). IGF-1 and HGF-mRNAs increased more significantly in the ventral midbrain of the cytokine group than in the ventral midbrain of the saline group. IL-1β and TNFα mRNAs markedly increased in the saline group, but the levels in the cytokine groups returned to the sham level. Immunohistochemical staining using anti-IL-1β and TNFα antibodies showed the positive immunostaining of the proinflammatory cytokines in DArgic neurons (blue arrowheads) and microglia (yellow ones) (Fig. 4C–F). In spite of such functional differences, microglial cells in the SNpc displayed amoeboid morphology in both the 6-OHDA-treated groups.

Contact between neurons and glia

Detailed morphological observation using 3D-constructed images taken by CLSM revealed the intimate contacts between neurons and glial cells and the presence of Iba1$^+$/NG2$^+$ cells (Fig. 5). The brain section in Figure 5 was from a cytokine-injected rat that was immunostained with antibodies to Iba1, NG2, and TH. The merged image of Iba1 and NG2 immunoreactivities (Fig. 5D) shows the presence of Iba1$^+$/NG2$^+$ cells, which have been described as a neuroprotective cell type (Kitamura et al. 2010). Activated microglial cells have long been described to intimately attach to damaged neurons and remove synaptic inputs. This phenomenon is called "synaptic stripping" and is supposed to be neuroprotective (Cullheim and Thams 2007; Trapp et al. 2007). The presence of synaptic stripping by immunofluorescence would be evident when the green fluorescence representative of Iba1-immunoreactivity is merged with the red fluorescence of TH-immunoreactivity, thus producing yellow color. Indeed, the merged yellow color is evident in the region where microglia and DArgic neurons intimately attach in Fig. 5E. In addition, NG2 glia also appeared to closely attach to DArgic neurons. This is seen when green immunofluorescence of NG2 is merged with the red immunofluorescence of DArgic neurons; the contact regions of NG2 glia and DArgic neurons appear as orange regions (Fig. 5F). The attachment of NG2 glia to DArgic neurons appeared more frequently than that of microglia.

Morphometric analyses of cell densities and interactions between glial cells and DArgic neurons

For the statistical evaluation of the cell types in the different treatments, detailed morphometric analyses were conducted using the CLSM images of Iba1, NG2, and TH immunofluorescence. Because immunoblotting and qRT-PCR was done on dissected ventral midbrain that not only contained the SNpc, but also other regions, it was necessary to employ immunohistochemical technique to analyze specific reactions of cells selectively in the SNpc. The region containing TH-immunoreactivity was defined as the SNpc region, and the area was determined using ImageJ 1.43u software. Similarly, areas containing TH, Iba1, and NG2 immunoreactivities were also independently measured. Furthermore, the following overlapping stained areas were also measured: TH/Iba1-double-positive areas (indicative of synaptic stripping by microglia), Iba1$^+$/NG2$^+$-double-positive areas (indicative of NG2$^+$ microglia), Iba1$^-$/NG2$^+$ areas (indicative of NG2 glia that are not microglia), and TH$^+$/Iba1$^-$/NG2$^+$ areas (indicative of attachment of NG2 glia to DArgic neurons). These areas were further divided by areas positive for SNpc, TH, or Iba1. Figures 6 A–C show examples of processed pictures from these morphometric analyses.

Summaries of the results obtained from the sham group (five rats) and the saline and cytokine groups (six rats) are shown in Figures 7A–G. TH/SNpc data are indicative of the number of surviving DArgic neurons in the SNpc (Fig. 7A), which was comparable to the immunoblot and RT-PCR data shown in Figure 1D–F. Cytokine injection significantly prevented DArgic neuronal loss. Iba1/SNpc is indicative of microglial activation (Fig. 7B). However, the Iba1$^+$ area in the SNpc was not markedly expanded, even in the 6-OHDA-treated rats, in spite of the presence of activated microglia. Furthermore, there was no difference in the Iba1$^+$ area between the saline and cytokine groups. TH+Iba1/TH is indicative of synaptic stripping (Fig. 7C), but there were no significant differences among the three groups. Total NG2/SNpc is indicative of the degree of activation and/or proliferation of NG2$^+$ cells, which includes NG2$^+$ microglia (Fig. 7D). This index significantly increased only in the cytokine group. The level of Iba1+NG2/Iba1 significantly increased in the 6-OHDA-treated rats as described elsewhere (Kitamura et al. 2010), both in the saline and cytokine-treated groups (Fig. 7E), suggesting that NG2$^+$ microglia do not

© 2011 The Authors. Published by Wiley Periodicals, Inc.

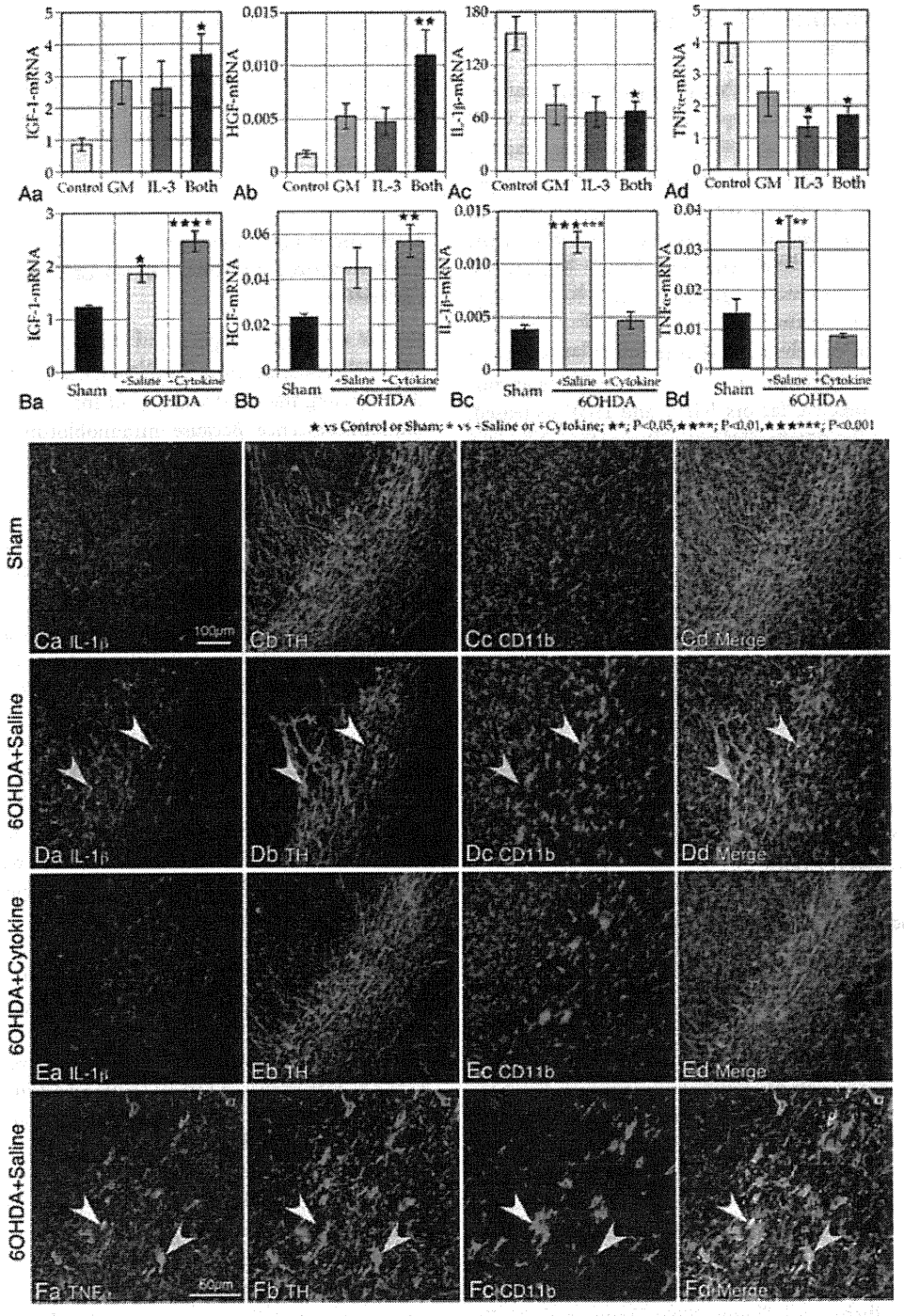

Figure 4. Effects of cytokines on microglial cells *in vitro* and *in vivo*. (**A**) qRT-PCR revealed that cultured microglial cells have increased mRNAs encoding IGF-1 (**Aa**) and HGF (**Ab**), while there is decreased mRNAs encoding IL-1β (**Ac**) and TNFα (**Ad**), when they were incubated with the cytokine mixture. The *in vitro* data were obtained from four separate cultures and expressed as means ± SEM. (**B**) mRNAs encoding IGF-1 (**Ba**) and HGF (**Bb**) also increased in tissue containing SNpc in response to the cytokine injection. By contrast, mRNAs for IL-1β (**Bc**) and TNFα (**Bd**) increased only in the saline group. *In vivo* qRT-PCR was from seven rats and expressed as means ± SEM. (**C–E**) IL-1β immunoreactivity in the SNpc of sham (**C**), saline (**D**), and cytokine (**E**) group at 1 week after 6-OHDA administrations. Rather strong IL-1β immunoreactivity was localized in neurons (blue arrowheads) and microglia (yellow arrowheads) in SNpc of saline-injected rats. (**F**) TNFα immunoreactivity was found in microglial cells (yellow arrowheads) and in neurons (blue arrowheads) in SNpc of saline-injected rats.

© 2011 The Authors. Published by Wiley Periodicals, Inc.

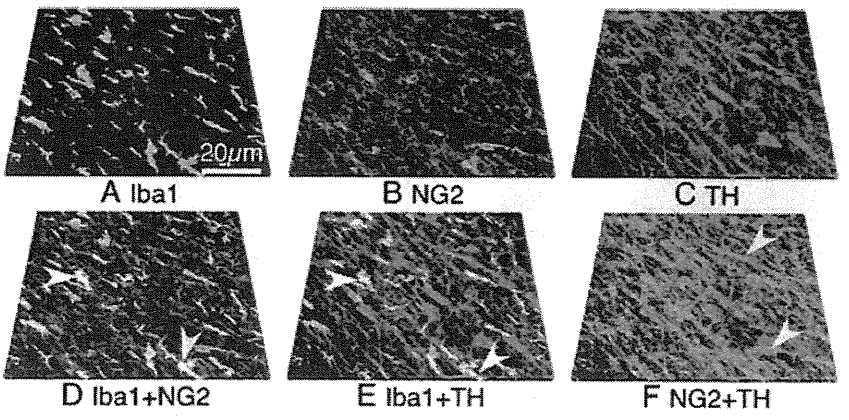

Figure 5. Reaction of cells expressing Iba1 and NG2 in the SNpc of a cytokine-injected 6-OHDA-administred rat, as shown in a 3D-reconstructed immunohistochemical picture. Seventeen 0.25-μm thick optical sections were reconstructed. (**A**, **B**, and **C**) Images show Iba1$^+$ (green), NG2$^+$ (pink), TH$^+$ (red) cells, respectively. (**D**) Iba1$^+$/NG2$^+$ cells, denoted with arrowheads, were present, displaying microglia-like morphology. (**E**) Iba1$^+$ microglial cells often are closely attached to TH$^+$ DA neurons (arrowheads), appearing as a merge of green and red colors to produce the yellow color. (**F**) Attachment of NG2$^+$ cells to TH$^+$ DA neurons. Color of NG2$^+$ cells was changed to green, and then merged with red colors. A closely attaching region between DA neurons and NG2$^+$ cells is displayed as an orange color (arrowheads).

contribute to the cytokine-induced DArgic neuronal survival. The NG2 alone/SNpc index increased only in the cytokine group (Fig. 7F), indicating that NG2 glia increased in number only in the cytokine group. TH+NG2 alone/TH index also increased only in the cytokine group (Fig. 7G). These morphometric data suggest that the increase of NG2 glial cell number and their attachment to DArgic neurons may underlie the neuroprotective effects of the cytokine mixture. mRNA encoding proliferating cell nuclear antigen (PCNA, a marker for proliferating cells) was markedly increased in the cytokine group, which may be indicative of increased NG2 glial cell numbers rather than microglia.

Astrocytes and astrocyte-related factors in the SNpc

Double-immunohistochemical staining using antibodies to GFAP and TH was done to evaluate astrocytes in the SNpc (Fig. 8). In the SNpc of the sham rats, GFAP immunoreactivity was scarcely distributed (Fig. 8A). In contrast, GFAP immunoreactivity was increased in the saline-injected rats (Fig. 8B). However, GFAP immunoreactivity was noticeably reduced in cytokine-injected rats (Fig. 8C). In agreement with these morphologic observations, GFAP-mRNA was also increased only in the saline group. mRNAs encoding BDNF, Cu/Zn SOD, and metallothionein 2, which could most likely be from astrocytes, were increased only in the saline group.

Discussion

This study demonstrated that subcutaneous administration of a cytokine mixture of GM-CSF and IL-3 exhibited marked neuroprotective effects against 6-OHDA-induced Parkinsonism in rats. It is of clinical relevance that the cytokine administration was started one day after the 6-OHDA-treatment. The dose of the cytokines was 10 μg/kg bodyweight, which is comparable to the dose of GM-CSF or IL-3 typically used for human cases to stimulate the bone marrow (Hocker et al. 1993; Bastion et al. 1995). Based on these facts, the cytokine mixture used in the present study may be clinically applicable for the treatment of PD. Furthermore, given the marked effects of this cytokine mixture in a model of PD, it can also be employed as a pharmacological tool to determine therapeutic targets to prevent PD-associated neuronal death.

Previously, it was shown that GM-CSF upregulates the expression of antiapoptotic factors belonging to the Bcl family in neurons expressing GM-CSFR (Huang et al. 2007; Schabitz et al. 2008), which resulted in the prevention of neuronal cell death. IL-3 was also shown to suppress neurodegeneration through increased Bcl-xL expression (Wen et al. 1998). In this study, subcutaneous injection of the cytokine mixture induced DArgic neurons in 6-OHDA-lesioned brains to upregulate Bcl-xL expression. This effect was independent of activated microglia, because DArgic neurons in the contralateral SNpc also upregulated expression of Bcl-xL, as shown in Figure 3. This likely contributed to suppressed DArgic neurodegeneration. The surviving neurons with elevated Bcl-xL expression then would affect the actions of glial cells within their vicinity. Neurons fated to die may activate microglial cells to accelerate neuronal degeneration, while surviving neurons may activate neuroprotective attributes of glial cells (Streit et al. 1999; Cullheim and Thams 2007).

© 2011 The Authors. Published by Wiley Periodicals, Inc.

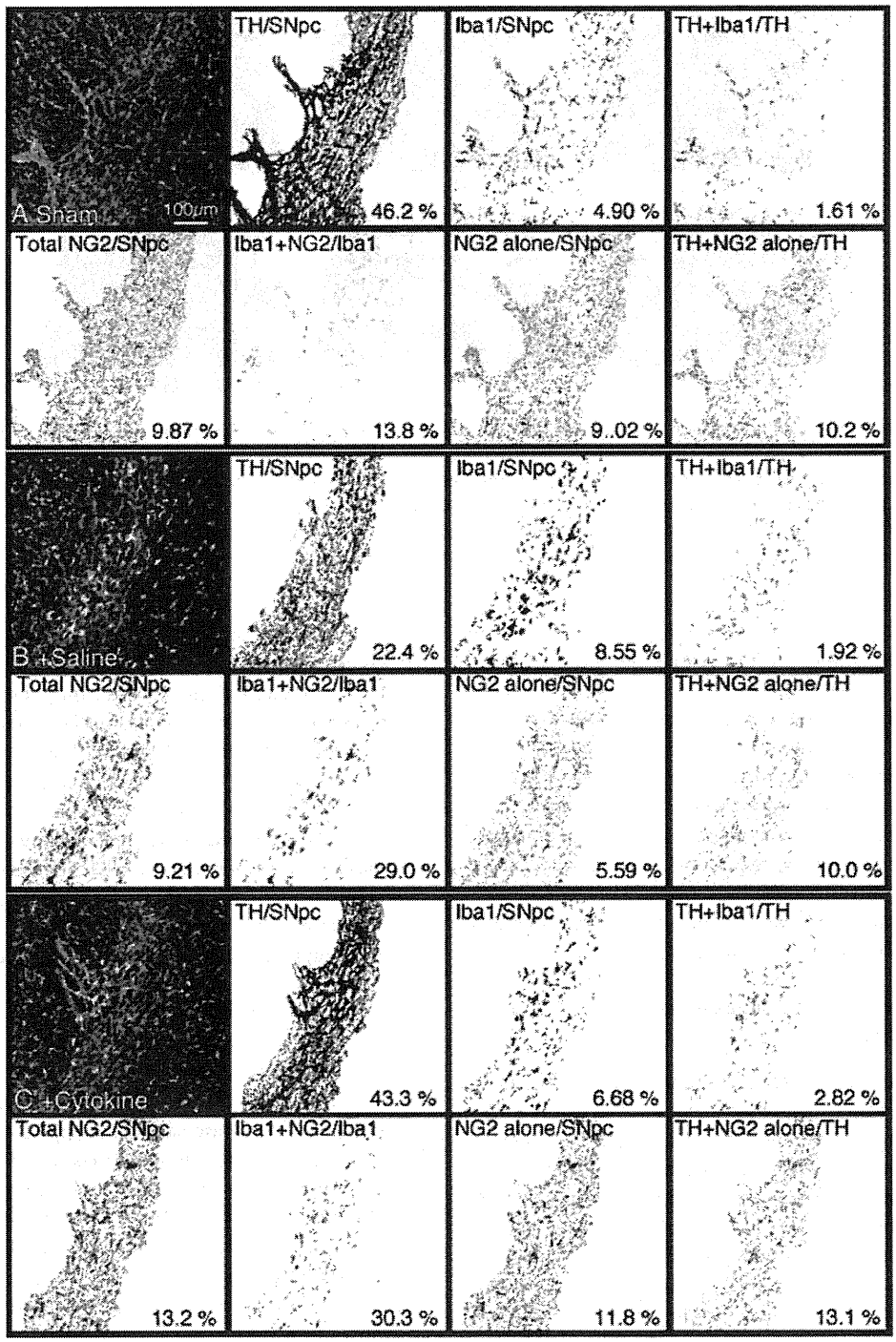

Figure 6. Morphometric analyses of TH^+, $Iba1^+$, and $NG2^+$ cells in the SNpc of sham, saline, and cytokine-treated rats. (**A**, **B**, and **C**) Images show triple-immunostained SNpc of each group of rats (at 1 week) with antibodies to TH (red), Iba1 (green), and NG2 (pink) as merged pictures. Black and white images were drawn from the original micrographs with individual colors, after SNpc regions were picked out, based on the distribution of the TH^+ DArgic neurons. TH/SNpc = ratio of TH^+ region in the SNpc. Iba1/SNpc = ratio of $Iba1^+$ region in the SNpc. TH+Iba1/TH = ratio of $TH^+/Iba1^+$ region in the TH^+ region, an index of synaptic stripping by microglia. Total NG2/SNpc = ratio of $NG2^+$ region in the SNpc. Iba1+NG2/Iba1 = ratio of $Iba1^+/NG2^+$ region in the $Iba1^+$ region, an index of the incidence of $Iba1^+/NG2^+$ cells. NG2 alone/SNpc = ratio of $NG2^+/Iba1^-$ region in the SNpc, an index of the incidence of $NG2^+$ cells that do not express Iba1. TH+NG2 alone/TH = ratio of $TH^+/NG2^+$, but not $Iba1^+$ region in the TH^+ region, an index of attached $NG2^+$ cells, but not microglia, to neurons.

© 2011 The Authors. Published by Wiley Periodicals, Inc.

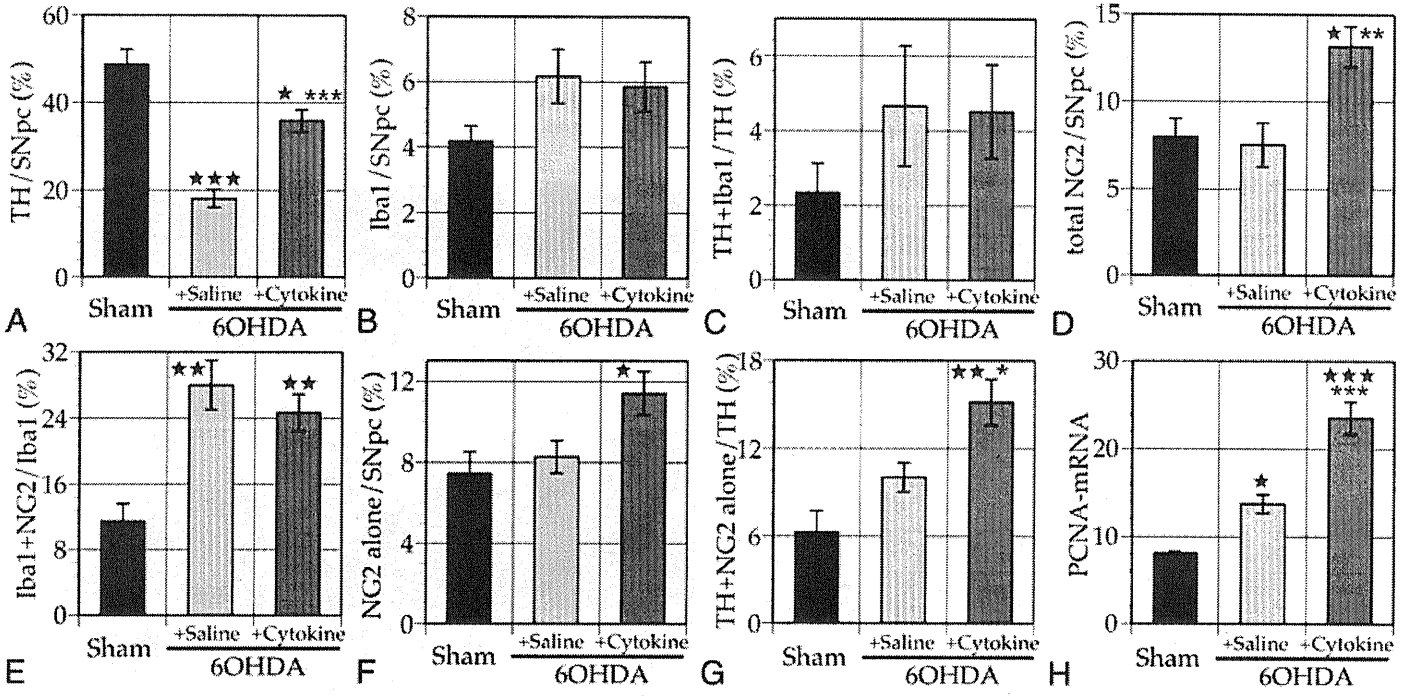

Figure 7. Based on the processed micrographs as shown in Figure 6, the morphometrical data from the sham group ($n = 5$) or saline ($n = 6$) and cytokine groups ($n = 6$) were statistically analyzed and expressed as means ± SEM. PCNA-mRNA level are also shown. (**A**) TH-immunoreactivity detected in the cytokine group was intermediate among the three groups. (**B**) In the SNpc, an increase of the Iba1$^+$ region, which is an index of microglial activation, was not significant in the Parkinsonian rats. (**C**) TH$^+$/Iba1$^+$ region, which is an index of synaptic stripping by microglia, was also not significantly increased. (**D**) Total NG2$^+$ region was increased in the cytokine group. (**E**) Iba1$^+$/NG2$^+$ region, which is an index of NG2$^+$ microglia, was increased in both the saline and cytokine groups. (**F**) NG2$^+$ cells that are not microglia increased in the cytokine group. (**G**) Cytokine injection increased TH$^+$/NG2$^+$ alone region occupied total TH$^+$ region, which is an index of NG2 cell attachment to DArgic neurons. (**H**) PCNA-mRNA level was elevated in 6-OHDA-treated rats, but the elevation was more significant in the cytokine group.

© 2011 The Authors. Published by Wiley Periodicals, Inc.

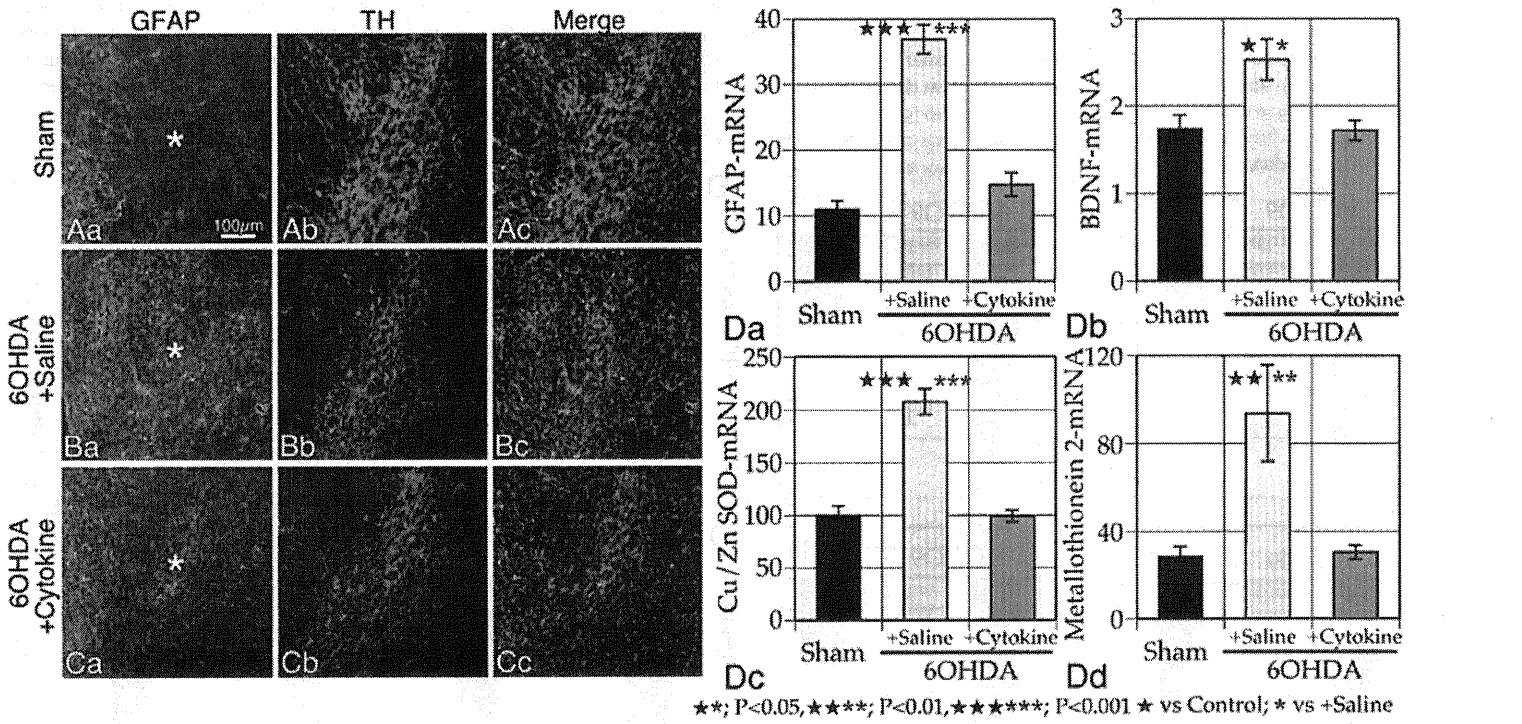

Figure 8. Reaction of astrocytes in the SNpc. (**A**) GFAP-immunoreactivity was weak in the SNpc (denoted with an asterisk) of sham-treated rats. (**B**) Strong GFAP-immunoreactivity was observed in saline-injected rats. (**C**) Moderate GFAP-immunoreactivity was observed in cytokine-injected rats. (**D**) mRNA levels encoding factors related to astrocytes as determined by real-time RT-PCR. GFAP-mRNA increased in the saline-injected group (**D**a). BDNF- (**D**b), Cu/Zn SOD- (**D**c), and metallothionein 2 (**D**d) mRNAs also increased in the saline-injected group. The data were obtained from seven rats.

© 2011 The Authors. Published by Wiley Periodicals, Inc.

Regardless of the cause of brain injury, microglial cells respond to even minor pathologic events in the brain, evident by morphologic changes such as enlargement of their cell bodies and shortening of their ramified processes (Kreutzberg 1996; Streit et al. 1999). 6-OHDA-treatment caused microglial activation with these types of morphologic changes. However, it is notable that the activated morphology was observed regardless of the survival of DA neurons, with or without the cytokine mixture injection. Interestingly, many studies have described the harmful effects of activated microglia on neurons (Mosley et al. 2006; Long–Smith et al. 2009; Tansey and Goldberg 2010); however, our results suggest that this may not always be the case.

There are some controversies regarding the activation of microglia (Liberatore et al. 1999; Henry et al. 2009; Marinova–Mutafchieva et al. 2009). Is their activation the cause or the result of DArgic neurodegeneration? Because DArgic neurodegeneration induced by 6-OHDA is a rather chronic process (Henry et al. 2009; Marinova–Mutafchieva et al. 2009), it is conceivable that microglial activation may influence the fate of DArgic neurons even if the DArgic neurodegeneration precedes microglial activation. In fact, proinflammatory cytokines, such as IL-1β or TNFα, and reactive oxygen species, such as NO or superoxide, which are produced by microglia, have been implicated in the pathogenesis of PD (McGeer and McGeer 2008; Long–Smith et al. 2009; Yacoubian and Standaert 2009; Tansey and Goldberg 2010).

The ameliorative effects of the cytokine mixture may be related to the functional changes of the activated microglia. The cytokine injection decreased the expression of IL-1β or TNFα in the SNpc of 6-OHDA-treated rats and it simultaneously increased expression of IGF-1 and HGF. IGF-1 (Guan et al. 2000; Ebert et al. 2008;) and HGF (Koike et al. 2006) have been shown for its ameliorative effects of 6-OHDA-induced rat Parkinsonism. Addition of GM-CSF and IL-3 to primary microglial cell cultures induced similar expression spectra of the proinflammatory cytokines and the neuroprotective factors. Thus, the action of the cytokine mixture to alter the microglial phenotype from a neurotoxic phenotype to a neuroprotective one, could at least partly explain the amelioration of 6-OHDA-induced Parkinsonism by the cytokine mixture. Damaged DArgic neurons can cause microglial activation through soluble factors, such as μ calpain (Levesque et al. 2010), and other insoluble factors on the plasma membrane (Sudo et al. 1998). Microglia activated by signals from damaged neurons may produce harmful factors that further contribute to neurodegeneration, or by phagocytizing the dying neurons. However, when the neuronal damage is not severe enough to induce neuronal death, microglia may become neuroprotective and promote neuronal survival by releasing various neuroprotective factors. This duality of function by microglia has long been proposed (Kreutzberg 1996; Streit et al. 1999; Cullheim and Thams 2007), and agents that change the microglial phenotype from destructive to protective have been sought for a long time as treatments for neurological disorders. This cytokine mixture may have this microglial phenotype-changing activity. The beneficial effect of this cytokine mixture may also be related to its ability to increase the expression of Bcl-xL in neurons. This effect may promote the survival of damaged neurons, activate the neuroprotective actions of surrounding microglia, and further bolster neuronal survival.

Expression of NG2 by microglia may be another hallmark of their activation (Yokoyama et al. 2006; Kitamura et al. 2010; Zhu et al. 2010). Although NG2$^+$ microglia have been reported to express a neuroprotective factor, GDNF (Kitamura et al. 2010), it appears that in the present scenario this neuroprotective factor did not contribute to neuronal survival in the 6-OHDA-induced Parkinsonism model. This is because NG2$^+$ microglia were present following 6-OHDA treatment without and with cytokine treatment.

6-OHDA-induced neurotoxicity has been attributed to oxidative stress (Glinka et al. 1997). Astrocytes have strong antioxidant properties (Tanaka et al. 1999; Miyazaki et al. 2011), and activated astrocytes are known to prevent DArgic neurodegeneration (Asanuma et al. 2010; Choudhury et al. 2011). Activated astrocytes were also evident in this study and the expression of mRNAs encoding Cu/Zn SOD and metallothionein 2, both of which play critical roles in suppressing oxidative stress, were upregulated in parallel with increased GFAP expression in the SNpc of the saline group. However, the activation of astrocytes and the upregulation of antioxidant factors did not lead to improved survival of neurons. Furthermore, when neurodegeneration was suppressed with the cytokine mixture, both astrocytic activation and the expression of antioxidative factors were also suppressed, suggesting that astrocytes and the antioxidative factors do not contribute to DArgic neuronal survival in the presence of the cytokines.

On the other hand, NG2 glia may contribute to the survival of DArgic neurons. NG2 glia are abundantly distributed throughout the brain and the spinal cord, representing 5–15% of nonneuronal cells (Staugaitis and Trapp 2009; Trotter et al. 2010). Some of these cells are also oligodendrocyte progenitor cells. However, it is not clear so far how these cells respond to neural injury in PD. As shown in the present study, NG2 glia appeared to increase in number and to attach intimately to damaged DArgic neurons in the SNpc in the cytokine group. Elevation of PCNA-mRNA may be related to the proliferation of NG2 glia. In contrast to astrocytes, the increase in the occupying area by NG2 glia and their attachment to DArgic neurons were prominent in the cytokine group, and therefore, it is possible that NG2 glia elicit neuroprotective effects under the influence of the cytokine mixture. However, NG2 glia did not express receptors for GM-CSF, and IL-3. NG2 glia may respond to IGF-1 and HGF

© 2011 The Authors. Published by Wiley Periodicals, Inc.

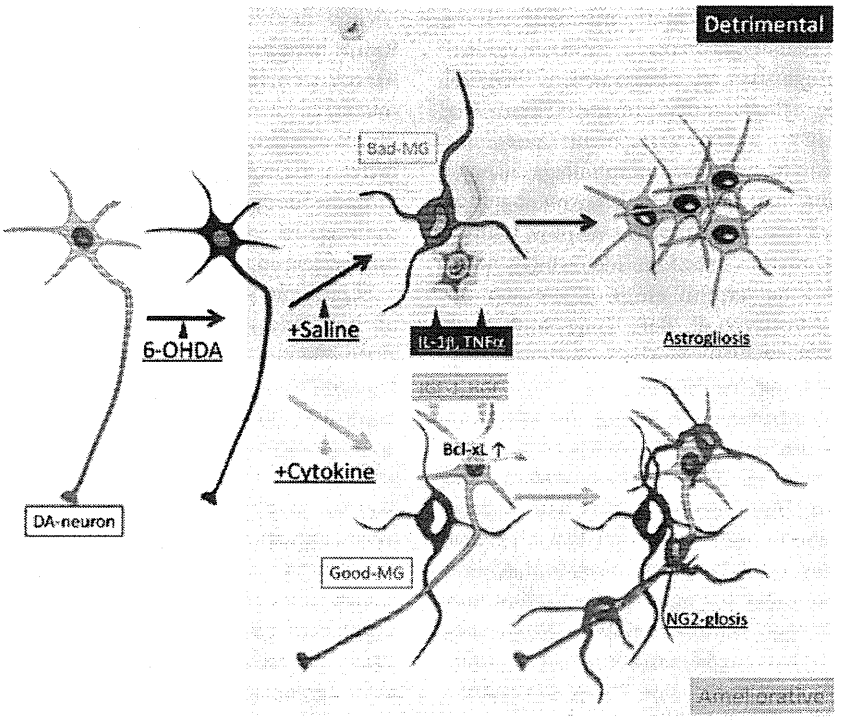

Figure 9. A summarized scheme based on the present data. 6-OHDA-induced DArgic neurodegeneration accompanies microglial activation. Without the cytokine mixture injection, activated microglia (MG) release the proinflammatory cytokine IL-1β and TNFα, causing further damage to DA neurons, and results in the formation of astrogliosis. Therefore, the activated microglia in this case can be considered as "Bad MG." When the cytokine mixture is injected, increased Bcl-xL expression suppresses DA neurodegeneration, and activated MG does not cause appreciable release of detrimental proinflammatory cytokines, but neuroprotectants, such as IGF-1 and HGF. Therefore, they can be considered as "Good MG." IGF-1 and HGF from activated MG can cause activation and proliferation of NG2 glia.

released by microglia. IGF-1 has been shown to be crucial for the survival of NG2 glial cells (Sundberg et al. 2010). NG2 glia express c-Met/HGF receptor, and HGF promotes NG2 glial proliferation (Ohya et al. 2007). In the present study, the cytokine mixture was found to upregulate expressions of IGF-1 and HGF in cultured microglia and in microglia in the ventral midbrain. Therefore, the cytokine mixture may stimulate NG2 glial survival and proliferation through IGF-1 and HGF, which is released by microglial cells in the SNpc of the cytokine-treated rats.

In conclusion, this study demonstrated the neuroprotective effects of a cytokine mixture containing GM-CSF and IL-3. A summary of our findings is shown in Figure 9. We propose that 6-OHDA administration into the striatum causes DArgic neurodegeneration in the SNpc and accompanying microglial activation (Fig. 9). The activated microglia produce proinflammatory cytokines that cause further chronic neurodegeneration. This neurodegeneration may also cause further activation of microglia, which in this scenario is not neuroprotective. Thus, a vicious cycle of neuronal degeneration occurs (Levesque et al. 2010). On the other hand, when the cytokine mixture is injected, DArgic neurons increase Bcl-xL expression, and thus, these neurons avoid degeneration in the face of 6-OHDA toxicity. In this scenario, the microglia become activated and display an activated morphology, similar to that in the saline group, but in this case they suppress proinflammatory cytokine expression. The microglia in the cytokine mixture-treated group have enhanced expression of the neuroprotective factors IGF-1 and HGF. IGF-1 and HGF enhances not only the viability of neurons but also the survival and production of NG2 glia, which can contribute to neuronal survival. Therefore, it is proposed that this cytokine mixture has neuroprotective properties and could help in the treatment of PD.

Acknowledgments

We are grateful to Staffs in Animal Center for their gentle care to animals and to M. Shudou for his technical assistance to operate CLSM that belongs to INCS of Ehime University. This work was partly supported by the Ministry of Education, Culture, Sports, Science, and Technology, Japan and Grants

© 2011 The Authors. Published by Wiley Periodicals, Inc.

for scientific research (Program for Enhancing Systematic Education in Graduate School).

References

Asanuma, M., I. Miyazaki, F. J. Diaz-Corrales, N. Kimoto, Y. Kikkawa, M. Takeshima, K. Miyoshi, and M. Murata. 2010. Neuroprotective effects of zonisamide target astrocyte. Ann. Neurol. 67:239–249.

Bastion, Y., L. Campos, N. Roubi, J. Bienvenu, P. Felman, C. Dumontet, and B. Coiffier. 1995. IL-3 increases marrow and peripheral erythroid precursors in chronic pure red cell aplasia presenting in childhood. Br. J. Haematol. 89:413–416.

Block, M. L., L. Zecca, and J. S. Hong. 2007. Microglia-mediated neurotoxicity: uncovering the molecular mechanisms. Nature Rev. Neurosci. 8:57–69.

Butt, A. M., N. Hamilton, P. Hubbard, M. Pugh, and M. Ibrahim. 2005. Synantocytes: the fifth element. J. Anat. 207:695–706.

Choudhury, M. E., T. Moritoyo, M. Kubo, W. T. Kyaw, H. Yabe, N. Nishikawa, M. Nagai, S. Matsuda, and M. Nomoto. 2011. Zonisamide-induced long-lasting recovery of dopaminergic neurons from MPTP-toxicity. Brain Res. 1384: 170–178.

Clarkson, E. D., W. M. Zawada, K. P. Bell, J. E. Esplen, P. K. Choi, K. A. Heidenreich, and C. R. Freed. 2001. IGF-I and bFGF improve dopamine neuron survival and behavioral outcome in parkinsonian rats receiving cultured human fetal tissue strands. Exp. Neurol. 168:183–191.

Cullheim, S., and S. Thams. 2007. The microglial networks of the brain and their role in neuronal network plasticity after lesion. Brain Res. Rev. 55:89–96.

De Lella Ezcurra, A. L., M. Chertoff, C. Ferrari, M. Graciarena, and F. Pitossi. 2010. Chronic expression of low levels of tumor necrosis factor-alpha in the substantia nigra elicits progressive neurodegeneration, delayed motor symptoms and microglia/macrophage activation. Neurobiol. Dis. 37:630–640.

Dekundy, A., M. Lundblad, W. Danysz, and M. A. Cenci. 2007. Modulation of L-DOPA-induced abnormal involuntary movements by clinically tested compounds: further validation of the rat dyskinesia model. Behav. Brain Res. 179:76–89.

Dreyfus, C. F., X. Dai, L. D. Lercher, B. R. Racey, W. J. Friedman, and I. B. Black. 1999. Expression of neurotrophins in the adult spinal cord in vivo. J. Neurosci. Res. 56:1–7.

Ebert, A. D., A. J. Beres, A. E. Barber, and C. N. Svendsen. 2008. Human neural progenitor cells over-expressing IGF-1 protect dopamine neurons and restore function in a rat model of Parkinson's disease. Exp. Neurol. 209:213–223.

Fujita, H., J. Tanaka, K. Toku, N. Tateishi, Y. Suzuki, S. Matsuda, M. Sakanaka, and N. Maeda. 1996. Effects of GM-CSF and ordinary supplements on the ramification of microglia in culture: a morphometrical study. Glia 18:269–281.

Glinka, Y., M. Gassen, and M. B. Youdim. 1997. Mechanism of 6-hydroxydopamine neurotoxicity. J. Neural Transm. Suppl. 50:55–66.

Guan, J., R. Krishnamurthi, H. J. Waldvogel, R. L. Faull, R. Clark, and P. Gluckman. 2000. N-terminal tripeptide of IGF-1 (GPE) prevents the loss of TH positive neurons after 6-OHDA induced nigral lesion in rats. Brain Res. 859:286–292.

Henry, V., V. Paille, F. Lelan, P. Brachet, and P. Damier. 2009. Kinetics of microglial activation and degeneration of dopamine-containing neurons in a rat model of Parkinson disease induced by 6-hydroxydopamine. J. Neuropathol. Exp. Neurol. 68:1092–1102.

Hocker, P., K. Geissler, M. Kurz, A. Wagner, and K. Gerhartl. 1993. Potentiation of GM-CSF or G-CSF induced mobilization of circulating progenitor cells by pretreatment with IL-3 and harvest by apheresis. Int. J. Artif. Organs 16(Suppl 5):25–29.

Huang, X., J. K. Choi, S. R. Park, Y. Ha, H. Park, S. H. Yoon, H. C. Park, J. O. Park, and B. H. Choi. 2007. GM-CSF inhibits apoptosis of neural cells via regulating the expression of apoptosis-related proteins. Neurosci. Res. 58:50–57.

Kitamura, Y., M. Inden, H. Minamino, M. Abe, K. Takata, and T. Taniguchi. 2010. The 6-hydroxydopamine-induced nigrostriatal neurodegeneration produces microglia-like NG2 glial cells in the rat substantia nigra. Glia 58:1686–1700.

Koike, H., A. Ishida, M. Shimamura, S. Mizuno, T. Nakamura, T. Ogihara, Y. Kaneda, and R. Morishita. 2006. Prevention of onset of Parkinson's disease by in vivo gene transfer of human hepatocyte growth factor in rodent model: a model of gene therapy for Parkinson's disease. Gene Ther. 13:1639–1644.

Kreutzberg, G. W. 1996. Microglia: a sensor for pathological events in the CNS. Trends Neurosci. 19:312–318.

Levesque, S., B. Wilson, V. Gregoria, L. B. Thorpe, S. Dallas, V. S. Polikov, J. S. Hong, and M. L. Block. 2010. Reactive microgliosis: extracellular micro-calpain and microglia-mediated dopaminergic neurotoxicity. Brain 133:808–821.

Liberatore, G. T., V. Jackson-Lewis, S. Vukosavic, A. S. Mandir, M. Vila, W. G. McAuliffe, V. L. Dawson, T. M. Dawson, and S. Przedborski. 1999. Inducible nitric oxide synthase stimulates dopaminergic neurodegeneration in the MPTP model of Parkinson disease. Nature Med. 5:1403–1409.

Long-Smith, C. M., A. M. Sullivan, Y. M. Nolan. 2009. The influence of microglia on the pathogenesis of Parkinson's disease. Prog. Neurobiol. 89:277–287.

Lue, L. F., Y. M. Kuo, T. Beach, and D. G. Walker. 2010. Microglia activation and anti-inflammatory regulation in Alzheimer's disease. Mol. Neurobiol. 41:115–128.

Marinova-Mutafchieva, L., M. Sadeghian, L. Broom, J. B. Davis, A. D. Medhurst, D. T. Dexter. 2009. Relationship between microglial activation and dopaminergic neuronal loss in the substantia nigra: a time course study in a 6-hydroxydopamine model of Parkinson's disease. J. Neurochem. 110:966–975.

McGeer, P. L., and E. G. McGeer. 2008. Glial reactions in Parkinson's disease. Mov. Disord. 23:474–483.

Miyazaki, I., M. Asanuma, Y. Kikkawa, M. Takeshima, S. Murakami, K. Miyoshi, N. Sogawa, and T. Kita. 2011.

© 2011 The Authors. Published by Wiley Periodicals, Inc.

Astrocyte-derived metallothionein protects dopaminergic neurons from dopamine quinone toxicity. Glia 59:435–451.

Mosley, R. L., E. J. Benner, I. Kadiu, M. Thomas, M. D. Boska, K. Hasan, C. Laurie, and H. E. Gendelman. 2006. Neuroinflammation, Oxidative Stress and the Pathogenesis of Parkinson's Disease. Clin. Neurosci. Res. 6:261–281.

Nishihara, T., M. Ochi, K. Sugimoto, H. Takahashi, H. Yano, Y. Kumon, T. Ohnishi, and J. Tanaka. 2011. Subcutaneous injection containing IL-3 and GM-CSF ameliorates stab wound-induced brain injury in rats. Exp. Neurol. 229:507–516.

Ohya, W., H. Funakoshi, T. Kurosawa, and T. Nakamura. 2007. Hepatocyte growth factor (HGF) promotes oligodendrocyte progenitor cell proliferation and inhibits its differentiation during postnatal development in the rat. Brain Res. 1147:51–65.

Schaar, D. G., B. A. Sieber, C. F. Dreyfus, and I. B. Black. 1993. Regional and cell-specific expression of GDNF in rat brain. Exp. Neurol. 124:368–371.

Schabitz, W. R., C. Kruger, C. Pitzer, D. Weber, R. Laage, N. Gassler, J. Aronowski, W. Mier, F. Kirsch, T. Dittgen, et al. 2008. A neuroprotective function for the hematopoietic protein granulocyte-macrophage colony stimulating factor (GM-CSF). J. Cereb. Blood Flow Metab.: 28:29–43.

Staugaitis, S. M., and B. D. Trapp. 2009. NG2-positive glia in the human central nervous system. Neuron Glia Biol. 5:35–44.

Streit, W. J., S. A. Walter, and N. A. Pennell. 1999. Reactive microgliosis. Prog. Neurobiol. 57:563–581.

Sudo, S., J. Tanaka, K. Toku, J. Desaki, S. Matsuda, T. Arai, M. Sakanaka, and N. Maeda. 1998. Neurons induce the activation of microglial cells in vitro. Exp. Neurol. 154:499–510.

Sundberg, M., H. Skottman, R. Suuronen, and S. Narkilahti. 2010. Production and isolation of NG2+ oligodendrocyte precursors from human embryonic stem cells in defined serum-free medium. Stem Cell Res. 5:91–103.

Takahashi, H., H. Matsumoto, A. Smirkin, T. Itai, Y. Nishimura, and J. Tanaka. 2008. Involvement of heparanase in migration of microglial cells. Biochim. Biophys. Acta 1780:709–715.

Tanaka, J., K. Toku, S. Matsuda, S. Sudo, H. Fujita, M. Sakanaka, and N. Maeda. 1998. Induction of resting microglia in culture medium devoid of glycine and serine. Glia 24:198–215.

Tanaka, J., K. Toku, B. Zhang, K. Ishihara, M. Sakanaka, and N. Maeda. 1999. Astrocytes prevent neuronal death induced by reactive oxygen and nitrogen species. Glia 28:85–96.

Tansey, M. G., and M. S. Goldberg. 2010. Neuroinflammation in Parkinson's disease: its role in neuronal death and implications for therapeutic intervention. Neurobiol. Dis. 37:510–518.

Trapp, B. D., J. R. Wujek, G. A. Criste, W. Jalabi, X. Yin, G. J. Kidd, S. Stohlman, and R. Ransohoff. 2007. Evidence for synaptic stripping by cortical microglia. Glia 55:360–368.

Trotter, J., K. Karram, and A. Nishiyama. 2010. NG2 cells: Properties, progeny and origin. Brain Res. Rev. 63:72–82.

Wen, T. C., J. Tanaka, H. Peng, J. Desaki, S. Matsuda, N. Maeda, H. Fujita, K. Sato, and M. Sakanaka. 1998. Interleukin 3 prevents delayed neuronal death in the hippocampal CA1 field. J. Exp. Med. 188:635–649.

Yabe, H., M. E. Choudhury, M. Kubo, N. Nishikawa, M. Nagai, and M. Nomoto. 2009. Zonisamide increases dopamine turnover in the striatum of mice and common marmosets treated with MPTP. J. Pharm. Sci. 110:64–68.

Yacoubian, T. A., and D. G. Standaert. 2009. Targets for neuroprotection in Parkinson's disease. Biochim. Biophys. Acta 1792:676–687.

Yokoyama, A., A. Sakamoto, K. Kameda, Y. Imai, J. Tanaka. 2006. NG2 proteoglycan-expressing microglia as multipotent neural progenitors in normal and pathologic brains. Glia 53:754–768.

Zhu, L., J. Lu, S. S. Tay, H. Jiang, and B. P. He. 2010. Induced NG2 expressing microglia in the facial motor nucleus after facial nerve axotomy. Neuroscience 166:842–851.

© 2011 The Authors. Published by Wiley Periodicals, Inc.

愛媛医学　Vol. 30　No. 1　55～58　2011

症例報告

バンコマイシン血中濃度からMunchausen症候群が疑われた１例

森　蓉子[1)]，永井　将弘[2)]，田邉　奈千[2)]，矢部　勇人[2)]，西川　典子[2)]，野元　正弘[2)]

1）愛媛大学大学院脳とこころの医学分野　2）愛媛大学大学院病態治療内科学分野

A case of Munchausen Syndrome suspected based on an inexplicable blood concentration of Vancomycin

Yoko Mori[1)], Masahiro Nagai[2)], Nachi Tanabe[2)], Hayato Yabe[2)], Noriko Nishikawa[2)] and Masahiro Nomoto[2)]

1）Department of Neuropsychiatry, Neuroscience, Ehime University Graduate School of Medicine
2）Department of Neurology and Clinical Pharmacology, Ehime University Graduate School of Medicine

Summary

A 31-years-old woman repeatedly suffered from a septic fever for two months. Although she was treated with several kinds of antibiotics, effectiveness of the drugs was transient. We noticed that her blood concentration of vancomycin was inexplicable low. We suspected she may be discarding her antibiotics. Furthermore, based on the unusual pattern of fever and pulmonary microembolism detected by chest CT-scan, we also suspected that she had contaminated her intravenous catheter or injected foreign substances intentionally. After the intravenous catheter was removed, the fever declined. For these reasons, we have diagnosed Munchausen syndrome. Munchausen syndrome is a psychiatric disorder characterized by the following features : 1) feigned illness or self-induced illness, 2) pathological lying, 3) wandering from hospital to ('hospital hopper').

In this case, the blood concentration of vancomycin provided a clue to the diagnosis of Munchausen syndrome. It is necessary to take Munchausen syndrome into consideration when symptoms and laboratory results are inexplicable.

Key Words : Munchausen syndrome, unknown fever, blood concentration of antibiotics

緒　言

Munchausen症候群とは，症状の自己産出，放浪癖，空想虚言を三徴とし，身体症状や精神症状を捏造する虚偽性障害の中でも最も悪性で身体症状の優勢なタイプを言う[1)~3)]。致死的となることもいとわず自らを傷つけ，患者役割を演じることで医療者の庇護を得ることを目的とする精神疾患である[2)]。

患者自身が作り出す症状は発熱，喀血，吐血，下血，血尿などの捏造しやすい症状が一般的とされるが，その他にも感染症，胸腹部症状，神経症状，皮膚症状，精神症状など多岐にわたり，多くの診療科を渡り歩いていくことが多い。医療者は患者の作り出した症状に直面し，「あるはずのない疾患」に対し過度の検査や加療を行い，時には複数回の手術を行うこともある。しかし，本来の医療行為の盲点を突いたような本症候群を疑うことは難しく，また患者自身が作り出した症状であるという客観的証拠も得にくく，診断は非常に困難である。このため，本症候群の有病率や予後などの疫学的データは不十分であり，現在のところも，その精神病理像や具体的な治療法など解明されていない点が多い。

我々は，対麻痺，腸管運動障害で入院，その後敗血症を繰り返し，治療に難渋した症例を経験した。本症例は最終的にバンコマイシン血中濃度という他覚的なデータからMunchausen症候群と診断するに到った。本症候群を診断するためには，医療者は時には「患者を

2010年９月15日受付　2010年11月30日採用

疑う」視点を持つ必要がある。

症　例

症　例：31歳　女性

主　訴：発熱

既往歴：腸炎の入院歴があるのみで，精神科通院歴はなかった。

家族歴：母が骨髄炎のため患者の幼少期より歩行障害あり。

家族背景：父母は離婚しており，患者は大学卒業後より地元を離れ独居していた。当科入院数ヶ月前に交際相手（医師）とのトラブルのため当地へ転居したばかりであった。

現病歴：X年9月初旬対麻痺・腸管運動障害にて当科入院。神経学的には両下肢4レベルの筋力低下，腱反射亢進，Th10レベル以下の感覚障害を認めた。排尿障害はなかったが，腸管麻痺を認めた。髄液検査，胸椎MRIにて異常は認めなかったが，下肢SEP，MEPは導出できず，脊髄炎を疑った。ステロイドパルス療法等を行うも症状の改善は認められなかった。高度の便秘があり，腹満感，嘔気・嘔吐を常時訴え，食事摂取困難であったため，偽性腸閉塞症状と考えて，経鼻胃管（NGチューブ）を挿入した。その後もNGチューブからの多量の排液があり腹部症状は軽快しなかった。12月初旬，栄養管理目的に中心静脈カテーテル(CVC)の留置を試みたが，留置困難であった。12月下旬CVCポート留置術施行。以降経口水分摂取制限の上，IVH管理していた。

X＋1年1月深夜，41度の発熱が出現した。

一般身体的所見：意識清明。身長：164.0 cm，体重：54.0 kg。血圧：100/54 mmHg，脈拍数：120/min，体温：41.0℃。ポート留置部の発赤・腫脹なし。眼瞼結膜：貧血なく，眼球結膜：黄疸なし。口腔所見：右C4にう歯を認めた。リンパ節：触知せず，肺音：清，心音：純・整，腹部：平坦・軟，肝脾触知せず，腸雑音正常であった。

神経学的所見：脳神経学的異常所見を認めず，徒手筋力検査では，上肢：3～4/5レベル，下肢：1～2/5レベルの筋力低下を認めた。深部腱反射は四肢で軽度亢進していたが，病的反射は認めなかった。感覚系は正常であった。

検査所見：血液検査においてWBC：14,000/ul（Stab：66%，Seg：19%，Lymph：6%，Mono：6%，Eosin：2%，Baso：1%），RBC：396万/ul，Hb：12.1 g/dl，Plt：13.7万/ul，CRP：13.87 mg/dl，β-Dグルカン：<6.0 pg/ml，プロカルシトニン：2.4 ng/mlと細菌感染症を示唆する所見を認めた。肝腎機能に異常を認めず，電解質も正常であった。不明熱の精査をおこなったが，腫瘍や膠原病を示唆する異常所見は認めなかった。

細菌検査では血液培養，喀痰培養から口腔常在菌であるα-Streptococcusが検出された。

全身CTでは炎症のfocusとなるような所見はなく，またイレウス像も認めなかった。

Gaシンチグラフィーにおいては炎症所見を認めなかった。

頭頸部CTでは脳内に異常所見を認めず，副鼻腔内に炎症所見は認めなかった。

上部消化管内視鏡検査にて異常所見を認めなかった。

経　過：経過図をFig. 1に示す。重症細菌感染症に対し，ただちにメロペネム投与を開始し，血液培養検査結果を受け，アミカシンの追加投与を行った。カテーテル感染症を疑ったが，腸管運動障害により絶食であること，CVC留置が非常に困難であったことを考慮し，しばらくの間CVCは抜去しなかった。しかし，抗生剤の効果を認めず，深夜に40℃を超える弛張熱が連日続いた。感染性心内膜炎なども疑ったが，心エコー検査では異常所見を認めなかった。やむを得ずCVCを抜去し，末梢静脈からタイペラシリン1日6回投与を開始した。数日の間は感染症の改善が見られたが，しばらくすると末梢ルート刺入部から血管の走行に一致した腫脹・発赤・疼痛を伴う静脈炎が出現するようになり，再度感染症が悪化した。留置針アレルギーや血管炎なども疑い精査を行ったが原因は明らかではなかった。

末梢静脈からの点滴が不可能となったため再度CVCを留置し，その後抗生剤をバンコマイシンに変更した。十分量を約1週間投与した後にバンコマイシン血中濃度を測定したところ，トラフ値：1.93 μg/ml（正常5以上），ピーク値：5.34 μg/ml（正常20以上）と血中濃度が異常に低いことが判明した。我々はこの時に初めて，抗生剤が確実に投与されていないのではないか，患者自身が抗生剤を破棄しているのではないかという疑いを持った。翌日より3日間，抗生剤投与中に医療スタッフがベッドサイドで付き添うことにより確

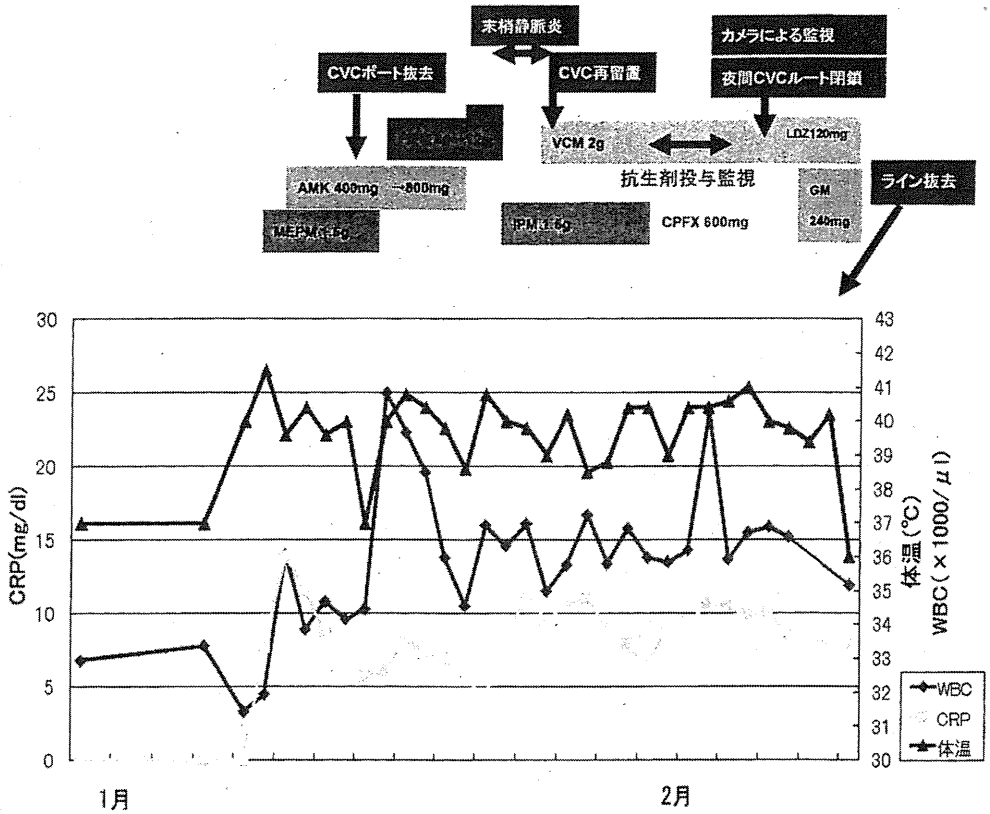

Fig. 1. Clinical course

実な投薬を行った。再度バンコマイシン血中濃度を測定したところ，トラフ値：6.36μg/ml，ピーク値：28.4μg/mlと，血中濃度の上昇を確認することができた。

胸部CTにおいて，両側全肺野に多発する0.5～2cm程度の結節影を認め（Fig. 2），何らかの原因による肺塞栓症が疑われた。

これらのことから，我々は患者自身が点滴ラインを操作し，治療薬を破棄したり，何らかの異物を注入して末梢静脈炎や菌血症を引き起こしたものと考えた。そこでカメラによる監視を開始した。この際，ベッド上での排泄中は撮影しないことで患者の同意を得た。また発熱は必ず深夜帯で出現していたことから夜間の静脈ラインの閉鎖も行った。翌日より深夜帯での発熱はなくなり，かわりに静脈ラインを開放している日中の排泄後のみに発熱が出現するようになった。これらの状況証拠から，本症例は感染症を自傷行為によって自己産出しているMunchausen症候群であると診断した。

このように，およそ40日間に渡り40℃を超える発熱が出現していた本症例であるが，CVCやNGチューブなどを抜去したところ，速やかに感染症は改善，以降発熱は完全に消失し，数日で抗生剤内服を中止できた。また，少量ずつ飲水や食事を開始したところ，腹部症状は出現しなかった。

その後感染症を引き起こすことができなくなった患者は，次々と演技的な手の巧緻運動障害や，足の対麻痺症状の悪化などを訴えるようになった。しかし精神科にコンサルテーションの上，家庭環境の整備と早期

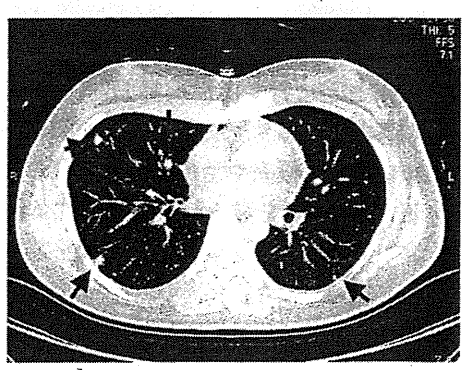

Fig. 2. Chest CT scan
The arrows indicate the embolisms.